Medium-Energy Neutron Time-of-Flight Spectrometer*

R. GRISMORE† AND W. C. PARKINSON
Harrison M. Randall Laboratory of Physics, University of Michigan, Ann Arbor, Michigan
(Received December 27, 1956, and in final form January 25, 1957)

A neutron time-of-flight spectrometer developed for the 1- to 20-Mev region is described. The instrument makes use of the phase bunching of deuterons in the Michigan 42-inch cyclotron and an external beam pulsing system to provide isolated bursts of neutrons of 4-mμsec time duration. Flight times are measured with an improved version of the chronotron capable of a precision of $\pm 3\times 10^{-10}$ sec. The energy spread for a 5-meter flight path varies from 3.5% at 0.5 Mev to 10% at 20 Mev. The available neutron flux permits an improvement of at least a factor of three by lengthening the flight path. The $Be^9(d,n)$ thick target and the $O^{16}(d,n)$ thin target spectra are discussed.

I. INTRODUCTION

A PROBLEM of long standing is the measurement of neutron energies in the Mev region with a resolution comparable to that obtainable for charged particles. The need for such a spectrometer is emphasized by the current state of the theory of nuclear structure, which in addition to predicting close-spaced levels asserts the correspondence of mirror nuclei and mirror reactions. Neutron spectrometers in the past have afforded energy spreads of the order of 10% above 1 Mev, although using nuclear emulsion techniques resolutions of a few hundred kev have been obtained. With the present state of accelerator technology, together with electronic techniques now available, time-of-flight spectrometers having comparatively high resolution are practicable.

The spectrometer described in this paper utilizes the phase bunching in the cyclotron to provide a narrow pulse of charged particles for the production of neutrons.[1] The neutron flight times are measured by means of an improved chronotron of timing precision $\pm 3\times 10^{-10}$ sec. The energy spread varies from 3.5% of the neutron energy at 0.5 Mev to 10% at 20 Mev. The neutron flux is sufficient to improve the resolution by at least a factor of three by extending the flight path. Because the method described here for recording data constitutes a limitation of the instrument, it is currently being modified for automatic recording without loss in resolution.

II. DESCRIPTION OF THE INSTRUMENT

A. General

A diagram of the instrument is shown in Fig. 1. Because of the phase-bunching action, 10^7 pulses of deuterons each of half-width 4 mμsec emerge from the cyclotron each second. One such pulse is allowed to strike the neutron-producing target every millisecond by applying an electrical pulse of width 10^{-7} sec, synchronized with the cyclotron oscillator, to a pair of deflection plates external to the cyclotron tank. The signal obtained when the deuterons strike the target serves as a timing marker for the formation of the neutrons. The 5.35-m flight path terminates in a liquid scintillation counter using 3 g/liter terphenyl in phenylcyclohexane with diphenylhexatriane added. The signals from the target and counter are coupled into opposite ends of the chronotron.[2]

A 55° magnet[3] focuses the pulsed deuteron beam onto the target with an energy spread of the order of 60 kev. The neutron beam is collimated by a water wall just beyond the target and by a cadmium-covered paraffin collimator 32 in. in diameter, 19 in. thick. The counter is shielded with 3 in. of lead and 6 in. of paraffin.

B. Pulsing System

A large positive dc potential applied to the upper of two plates (Fig. 2) to deflect the deuteron beam into a "catcher" is nullified by a pulse from the high-voltage pulser allowing one deuteron burst to reach the target. To reduce the neutron background the plates are tilted to prevent the beam striking their surfaces and to allow it to be stopped in the lead catcher.

To synchronize the pulser with the cyclotron dee oscillator the rf signal (10.2 Mc) from the oscillator is scaled down a factor of ten thousand in decade type scaling units and applied to a low-voltage driver pulser, which in turn triggers the high-voltage pulser. The firing point of the pulser can be varied over more than two cycles of the rf by means of a variable delay line between the decade units. In operation it is adjusted so that only one deuteron burst per deflection plate pulse is obtained.

The low-voltage pulser is a conventional hydrogen thyratron circuit using a type 3C45 tube with a plate line and produces a pulse of 800-volts amplitude and 0.6-μsec half-width. The high-voltage pulser (Fig. 3) produces an output pulse of triangular shape with rounded top

* This work was supported in part by the U. S. Atomic Energy Commission and in part by the Michigan Memorial Phoenix Project.
† Now at Argonne National Laboratory, Lemont, Illinois.
[1] Annual Report to U. S. Atomic Energy Commission under contract AT(11-1)-70 project #1, March 31, 1953, *et seq.*
[2] M. Newman, Phys. Rev. **52**, 652 (1937); Neddermeyer, Althaus, Allison, and Schatz, Rev. Sci. Instr. **18**, 488 (1947); J. Keuffel, Rev. Sci. Instr. **20**, 197 (1949).
[3] Bach, Childs, Hockney, Hough, and Parkinson, Rev. Sci. Instr. **27**, 516 (1956).

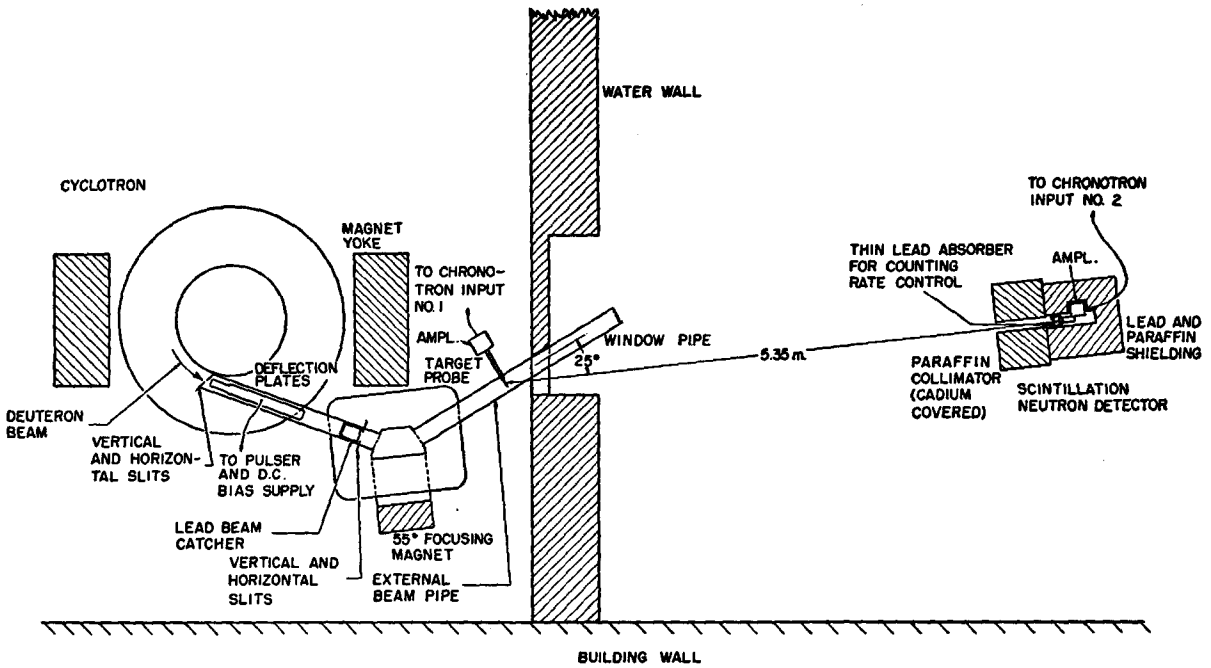

FIG. 1. Floor plan of apparatus for neutron time-of-flight.

of half-width 0.1 μsec and an amplitude variable from 0 to 40 kilovolts. In order to obtain the short pulse width with large amplitude a condenser bank in series with one section of an auto-transformer is connected across a hydrogen thyratron. A second hydrogen thyratron driven by the same trigger through a delay line is connected across a second section of the transformer and acts as a clamping device to bring the pulse to zero after the required width is obtained. The rise time of the output, taken from the third section of the transformer, is essentially determined by the constants of the pulse transformer and the small amount of resistance which the 5C22 retains in its fired condition. The 705 A diode is used as a voltage doubler.

The transformer was wound with a single layer of No. 22 d.c.c. copper wire on one side of an "O"-shaped core $4\frac{3}{4}$ in. long by 3 in. wide. The core has a 1 in. by $1\frac{3}{8}$-in. rectangular cross section and is made of a 2-mil hypersil sheets. Insulation was provided by a number of layers of varnished cambric. Time jitter in the firing of the pulser was made less than 10^{-8} sec by (1) using filtered dc power for the filaments of the 5C22 tubes,

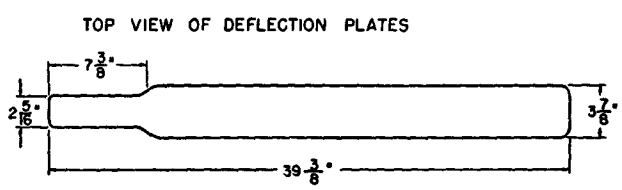

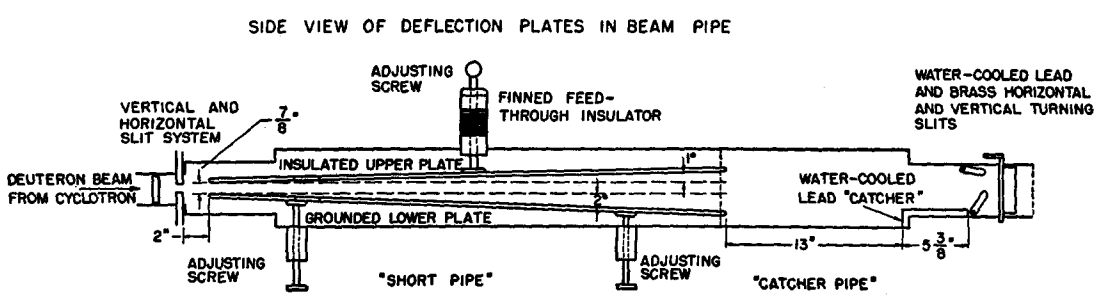

FIG. 2. Geometry of deuteron-beam deflection plates.

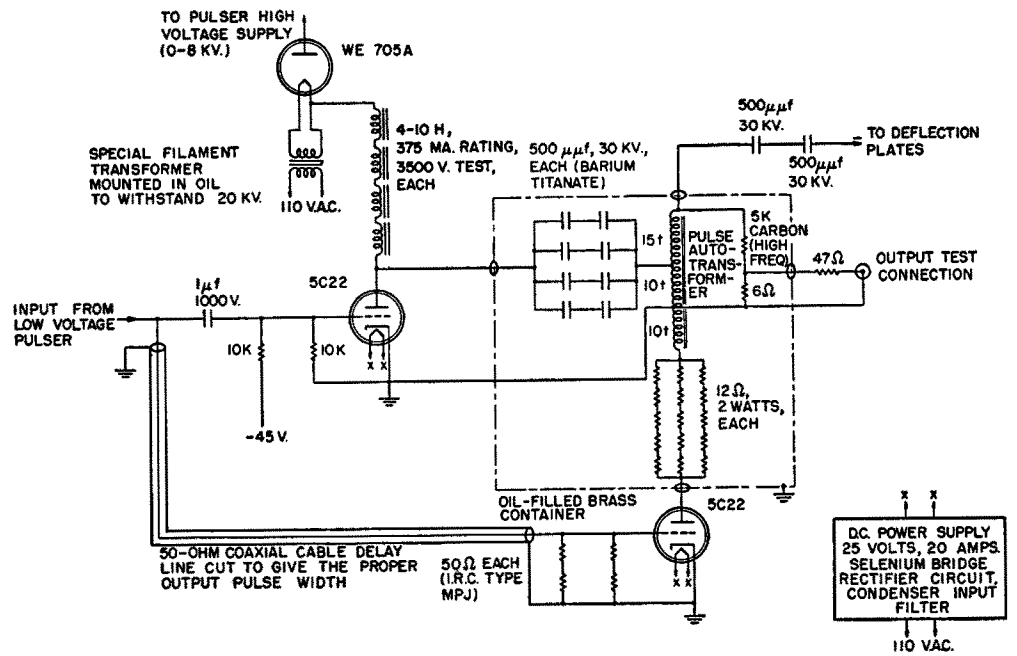

FIG. 3. Circuit diagram of high-voltage pulser.

(2) ensuring that the triggering pulse rises rapidly through the firing point of thyratrons, and (3) by maintaining a small grid-to-ground impedance of the tubes in the circuit.

C. Neutron Target and Detector

The probe which carries the target material forms a 200-ohm coaxial line, the center conductor of which terminates in a rectangular lead billet. The outer conductor, at the location of the billet, has two thin lead foil windows located diametrically opposite which allow the deuteron beam to reach the billet with small energy loss, and at the same time serve as electrostatic shields. The billet intercepts all the beam entering the window. The target material is placed on one of the lead foils. By rotating the probe 180° the pure foil can be exposed to the deuteron beam for measurement of the background. The thick target measurements reported below were made using a beryllium billet and aluminum foil windows.

The circuit associated with the probe is shown in Fig. 4. The resistances R_1 and R_2 were adjusted to give a pulse of half-width approximately 2×10^{-8} sec, the optimum width for use with the chronotron. The pulses are of the order of 10 mv in amplitude for the average pulsed beam intensity.

The unpulsed deuteron beam to the target is conveniently maximized by rotating an auxillary probe into a position directly in front of the target. The pulsed beam is maximized by measuring the amplified signal from the target probe with a vacuum tube voltmeter. Such an arrangement permits easy adjustment of the cyclotron and pulser for maximum counting rate.

A liquid scintillation counter, because of its high efficiency and short decay time, was used as a detector. Details of the container and of the type 5819 photomultiplier circuit are shown in Fig. 5. The output pulses were clipped to 2×10^{-8} sec by means of shorted 197-ohm coaxial line. The wide-band amplifier was located close to the anode of the photomultiplier to reduce stray shunt capacitance. With a 5.3-meter flight path the diameter of the container (4 in.) results in a solid angle of 2.8×10^{-4} steradian while the length (8 cm) causes an uncertainty in the flight path of $\pm0.7\%$.

D. Chronotron

The chronotron timing circuit shown in Fig. 6 is similar to that of Keuffel,[4] with several modifications. Coaxial cable of characteristic impedance 197 ohms[5]

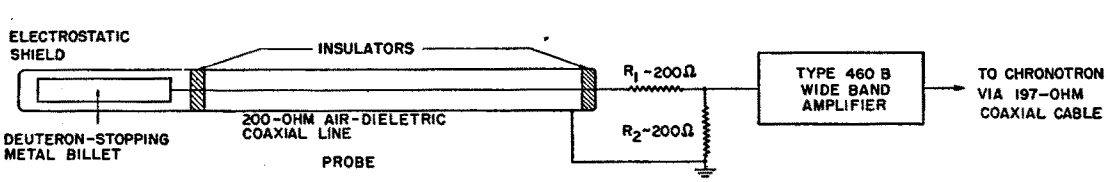

FIG. 4. Electrical circuit of target probe.

[4] Keuffel, Harrison, Godfrey, and Reynolds, Phys. Rev. 87, 942 (1952).
[5] Type C3-T manufactured by Transradio Limited, London, England.

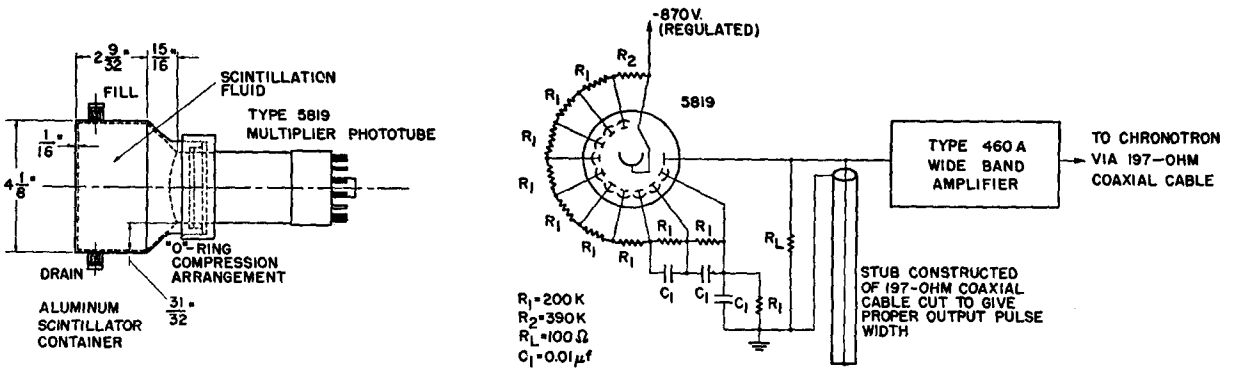

FIG. 5. Mechanical and electrical details of neutron detector.

was used in preference to two-wire open transmission line and the input pulse shapes are preserved thereby retaining the maximum information. A method of interpolating between detector stations was developed that permits the meeting point of the pulses to be determined to a small fraction of the detector spacing.

The signals from the probe and counter are amplified by wide-band distributed amplifiers to provide the required 2 to 3-volt undistorted signal. The output impedances of the last amplifiers in the probe and counter system are carefully matched to the impedance of the line to prevent reflections.

The detectors and the mixer unit, patterned after those used by Keuffel,[2] are shown in Figs. 7 and 8, respectively. The values of R_s and R_p at the detector input are dictated by the opposing requirements that the attenuation along the entire length of the line not exceed 0.6, (imposed by the system of interpolation), while approximately 0.1 of the input voltage be available for charging the capacitance in each detector. The connectors between the line and the detectors are designed to prevent reflection. For the values of R_s, R_p, and C used the charging time constant is

$$\tau=[\{(R_sR_p)/(R_s+R_p)\}+R_c]\cdot C=3\times10^{-9}\text{ sec},$$

where R_c is the forward resistance of the 1N56 crystal diode. Since τ is much less than the time of passage of a pulse past a detector, adequate discrimination is obtained between voltages applied separately and those applied simultaneously.

The trigger circuit of Fig. 6 gates on the oscilloscope trace only when a scintillation counter event of sufficient size occurs in the correct time relation with respect to a probe pulse. Discriminators at the inputs to the crystal bridge coincidence circuit control the minimum probe and counter pulse amplitudes accepted. Because the resolving time of the coincidence circuit is 2×10^{-7} sec while the chronotron range is 1.6×10^{-7} sec, some traces are photographed for which voltage maxima are not observed.

The method of interpolation is based on the adjustment of the widths of the probe and counter pulses so that their region of overlap on the chronotron will always affect two, but only two, adjacent detectors. Let

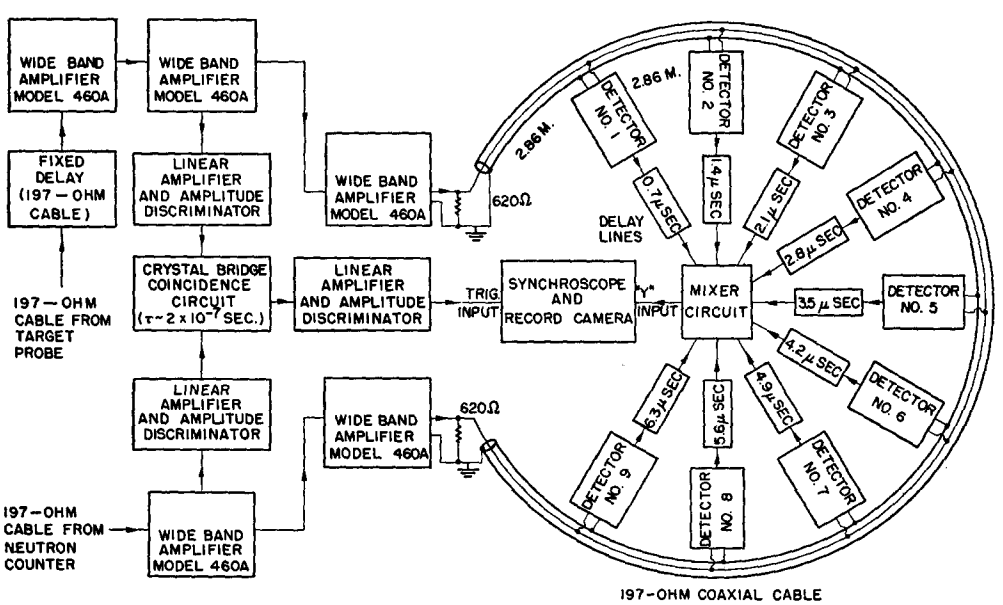

FIG. 6. Block diagram of chronotron.

Δ_1 and Δ_2 be the amounts by which the responses of the two detectors rise above the normal pattern. The ratio $R=\Delta_1/\Delta_2$ will then be a single-valued function of the distance of the pulse meeting point from either detector. If R is a known function of position, then the meeting point and from it the time difference of entry of the pulses into the chronotron can be obtained to a small fraction of the detector spacing.

The timing pulses were adjusted to be 2×10^{-8} sec in half-width, since this gives sufficient chronotron range with a reasonable number of detectors. A smaller width results in loss of amplitude of the counter pulses. With the detectors spaced 2.86 m apart, a shift of one detector spacing interval in the meeting point of a pair of pulses corresponds to a change of 20 mμsec in their time difference of entry into the chronotron. The interpolation is readily carried out to the nearest 0.1 of this.

The ratio R was measured as a function of the position of the pulse meeting point using the probe pulses for one input and the accompanying prompt gamma-ray counter pulses for the other. The meeting

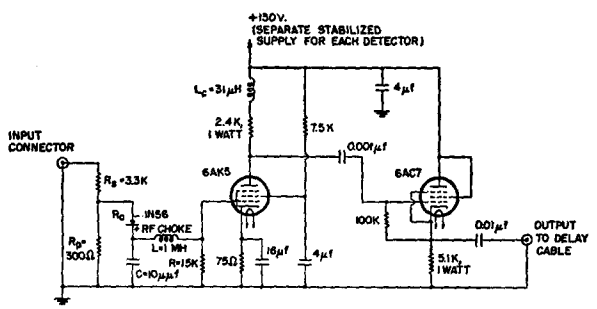

FIG. 7. Schematic diagram of chronotron detectors.

point was shifted by known amounts by inserting appropriate lengths of cable in one input circuit and the variation of R with position observed. A tracing of one such chronotron pattern is reproduced in Fig. 9. The results of a number of such observations are plotted to give the interpolation curve shown in Fig. 10. The lack of symmetry of the interpolation curve (Fig. 10) about the abscissa 0.5 is believed due to differences in shape of the probe and counter pulses.

The interpolation method places severe stability requirements on the detectors since any random fluctuation from the normal will be interpreted either as a meeting of two pulses or as a shift in a true meeting point. The detector components were carefully matched and many traces observed with only one input to the chronoton to determine the fluctuations in the detectors as the input amplitude was varied. Of some 350 traces measured, the probability of a detector fluctuation greater than 5% was about 1%.

The time resolution of the chronotron was determined using pulses from two type 5819 photomultipliers viewing the same stilbene crystal exposed to gamma

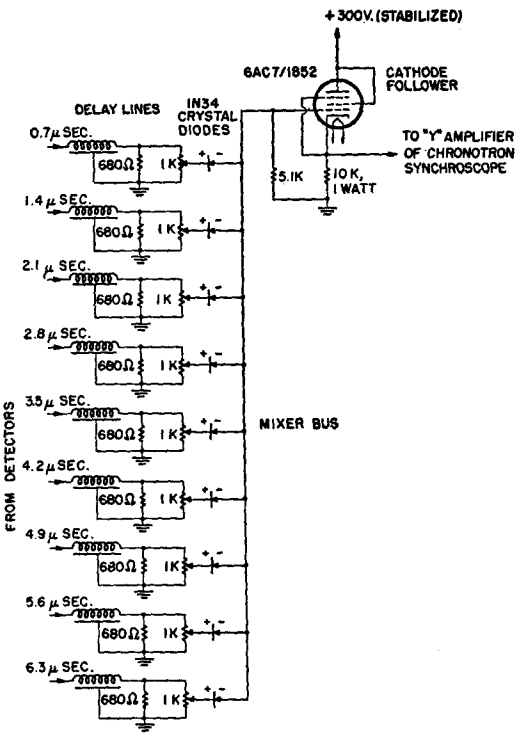

FIG. 8. Schematic diagram of chronotron mixer.

radiation. The distribution of values of the ratio R measured in this way is shown in Fig. 11. The mean half-width of several such distributions was $(7.0\pm0.5)\times10^{-10}$ sec. This implies a standard deviation of a single time measurement of $\pm3\times10^{-10}$ sec, and represents an upper limit for the precision of the present model of the chronotron. It is in reasonable agreement with the theoretical predictions of Morton,[6] which indicate a standard deviation of $\pm2.8\times10^{-10}$ sec, owing to time variations in the phosphor and the photomultiplier.

III. EXPERIMENTAL RESULTS

A. The Thick Target $Be^9(d,n)$ Spectrum

To test the operation of the spectrometer measurements were made using a thick beryllium target. The results obtained for two adjacent chronotron ranges are shown in Fig. 12.

The prompt gamma-ray peak is used as an energy calibration. The time resolution of the spectrometer, (the time difference between two equal intensity monoenergetic neutron groups which are just distinguishable) is given by the 4-mμsec half-width of the gamma peak

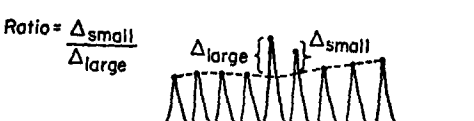

FIG. 9. Tracing of actual chronotron pattern.

[6] G. A. Morton, Nucleonics **10**, No. 3, 39 (A) (1952).

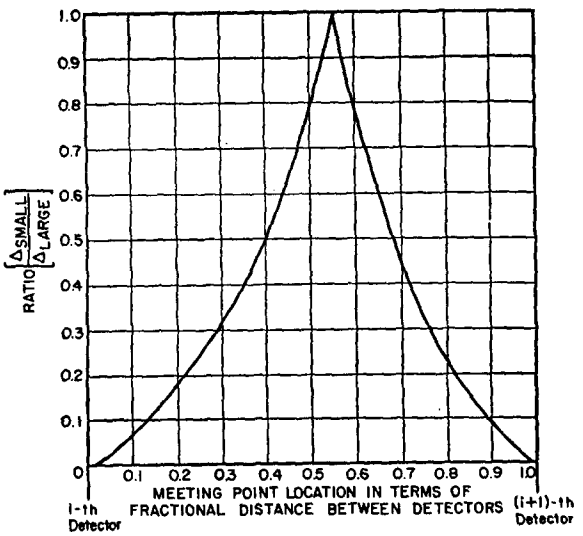

FIG. 10. Chronotron interpolation curve.

which is just the time duration of the deuteron bursts from the cyclotron. The resolution is somewhat less for neutron groups than for gamma rays because of the finite extent of the counter. Curves of the resolution as a function of neutron energy calculated assuming a deuteron burst width of 4-mμsec, a detector resolving time of 1 mμsec and a time spread in the photomultiplier of $\frac{1}{2}$ mμsec are plotted in Fig. 13 for two flight paths and two detector lengths. It does not include the effects of energy spread of the deuteron beam, energy loss in the target, or angle straggling of the neutrons from the solid angle of the counter.

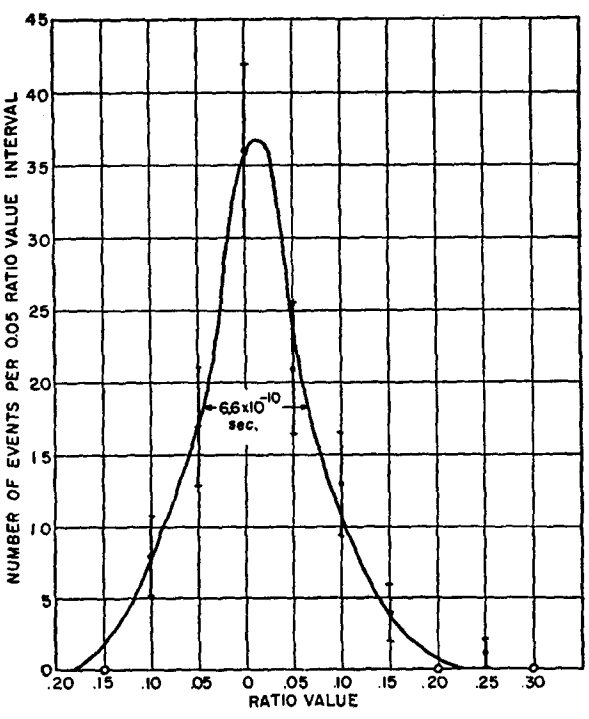

FIG. 11. Time resolution of chronotron.

The propagation velocity for the 197-ohm coaxial cable was calculated to be $(2.86\pm0.04)\times10^8$ m/sec from the line constants and was measured to be $(2.81\pm0.05)\times10^8$ m/sec from the separation of the gamma-ray peak and the Si^{28} ground-state neutron group. A mean value of $(2.84\pm0.02)\times10^8$ m/sec was adopted.

Certain features in the beryllium spectrum (Fig. 12) are of interest. Neutron groups associated with the ground, second, and third excited states of Si^{28} result from the (d,n) reaction on the aluminum window in front of the beryllium billet. The first excited state is not observed presumably because the first minimum of the angular distribution occurs near the angle of observation.[7] The broad group in the gamma spectrum (flight time $=5.5\times10^{-8}$ sec) and the sharp peaks at 3.7 and 5.8 Mev in the neutron spectrum have not been completely identified, although it has been shown that they are not due to peculiarities of the timing apparatus. The broad group would correspond to a neutron energy too high (55 Mev) to be due to any of the (d,n) reactions known, and it can be demonstrated by probability arguments that it cannot be due to "afterpulses" in the photomultiplier[8] or a double structure of the deuteron bursts. The best guess is that the group is due to gamma rays from deuterons striking some material in the ductwork due to improper adjustment of the beam deflection voltage. The sharp peaks at 3.7 and 5.8 Mev are too narrow to be due to either the aluminum window or the beryllium target. They are believed to be either neutrons from (d,n) reactions occurring on a contamination layer on the target, or to gamma rays such as those producing the broad group.

B. The $O^{16}(d,n)$ Spectrum

As a further test of the spectrometer the neutron spectrum resulting from deuteron bombardment of a lead dioxide target was measured. The reaction $O^{16}(d,n)F^{17}$ is of particular interest since levels above the first excited state have not been measured previously by means of the (d,n) reaction. While much is known[9,10] about the mirror nucleus O^{17} the location of the $(d_{\frac{3}{2}})$ single particle level in F^{17} has been left in doubt by (p,p) elastic scattering experiments.[11,12]

Data were taken corresponding to the excitation ranges 0 to 3.81 Mev and 4.64 to 4.93 Mev in F^{17}. Two targets of thicknesses 175 kev and 60 kev were used, and each was prepared by depositing chemically pure lead

[7] Calvert, Jaffe, Litherland, and Maslin, Proc. Phys. Soc. (London) 68A, 1008 (1955).
[8] Godfrey, Harrison, and Keuffal, Phys. Rev. 84, 1248 (L) (1951).
[9] F. Ajzenberg and T. Lauritsen, Revs. Modern Phys. 27, 77 (1955).
[10] T. S. Green and R. Middleton, Proc. Phys. Soc. London A69, 28 (1956); W. J. Childs and W. C. Parkinson (to be published).
[11] R. A. Laubenstein and M. J. W. Laubenstein, Phys. Rev. 84, 18 (1951).
[12] Sempert, Schneider, and Martin, Helv. Phys. Acta 27, 313 (1954).

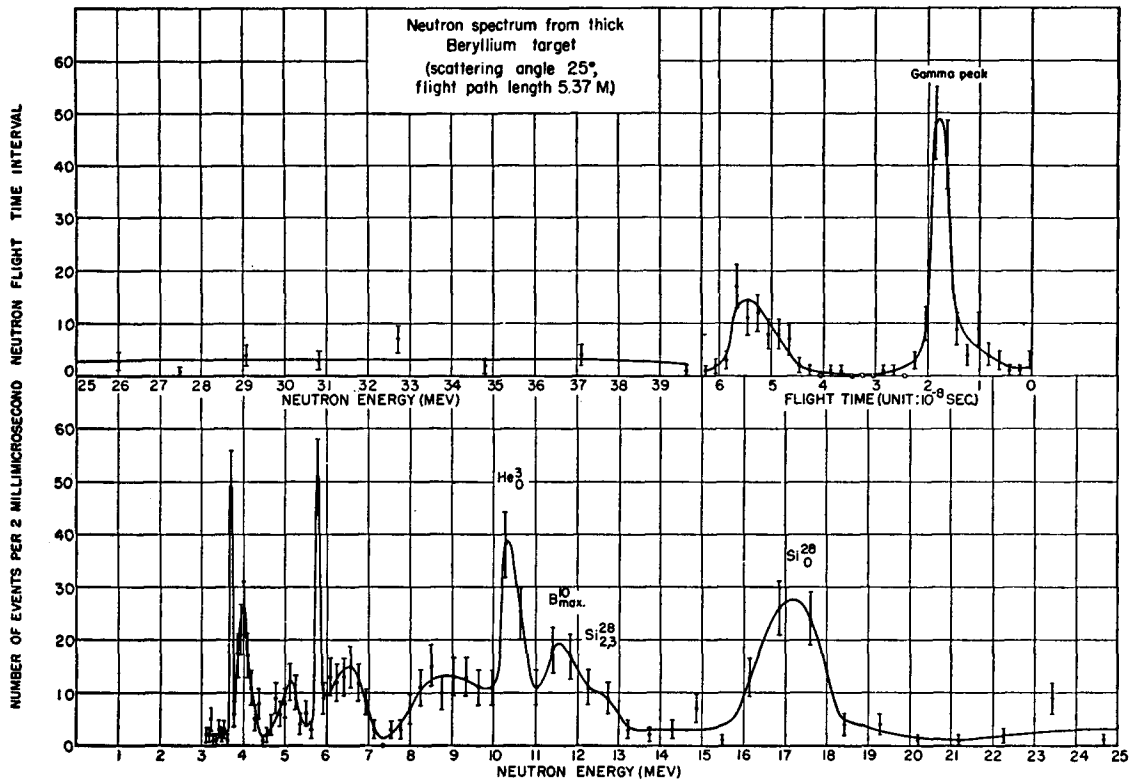

FIG. 12. The $Be^9(d,n)$ thick target spectrum.

dioxide onto the lead foil window of the target probe from an alchohol suspension. In the neutron energy range from 1.77 to 7.5 Mev the 175-kev target was used, and data were taken both with the lead dioxide target and with a plain lead target. The data included 1422 target events and 703 background events. The results

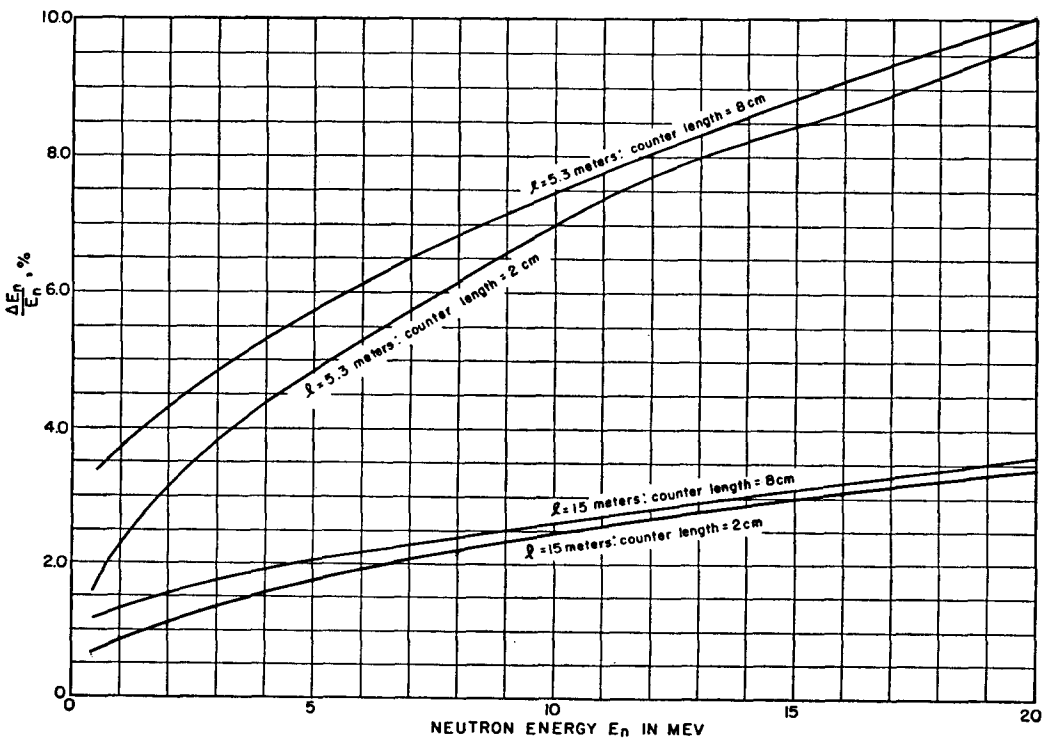

FIG. 13. Spectrometer resolution as a function of energy.

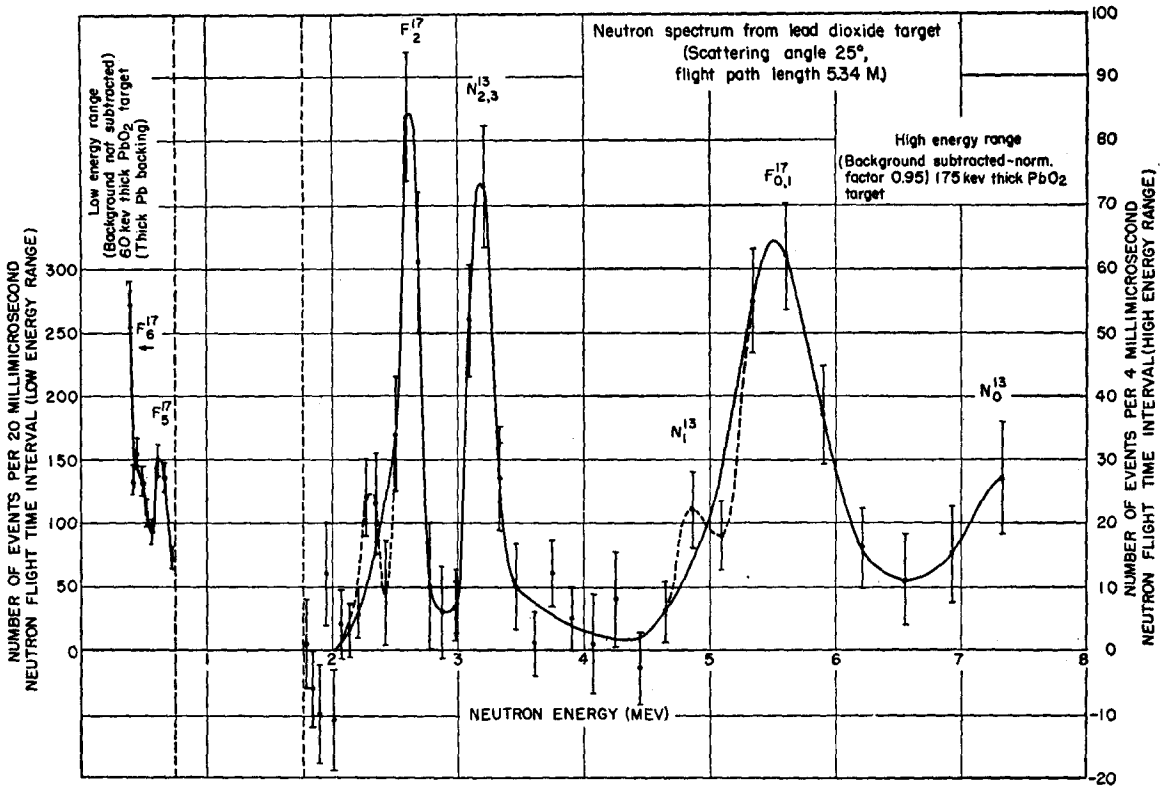

FIG. 14. The $O^{16}(d,n)$ spectrum.

after subtraction of the background are shown in Fig. 14. The bars indicate the standard deviations. Since the total current to the target was not measured, it was necessary to normalize the background data. This was done by minimizing the sum of the squares of the differences between corresponding points of the two curves in the regions of evident match. The data taken with the 60-kev target in the lower energy range is shown at the left of Fig. 14.

Neutron groups corresponding to all the previously known F^{17} levels within the given excitation ranges are evident in Fig. 14. In addition, groups are found corresponding to the $C^{12}(d,n)$ reaction occurring with carbon impurities in the targets. There is no evidence in the spectrum of new levels, except for a small elevation composed of two points at a neutron energy near 2.3 Mev.

The energy and half-widths measured for the well-defined groups are given in Table I, together with the known levels with which the groups have been identified. Included in the table is the half-width predicted for each group on the basis of the over-all spectrometer resolution, taking into account the uncertainty in the flight path and the deuteron energy loss in the target. Energy and angle straggling are too small to affect the resolution and were neglected. The spread in energy of the incident deuteron beam was not included since it has not been measured. However, the 90-kev half-width of the F_5^{17} group indicates that it must be somewhat less than 80 kev. The fact that the F_0^{17} and F_1^{17} groups are not resolved is believed due to the poor statistics which do not allow the use of sufficiently small energy channels. Since the predicted half-widths were calculated assuming a single neutron group, the level separations (499 and 50 kev, respectively) should be considered in comparing the calculated and observed values for the unresolved doublets $F_{0,1}^{17}$ and $N_{2,3}^{13}$. Considering the rather meagre statistics, the agreement between the measured and predicted values is surprisingly good.

The measured Q values and corresponding excitation energies are listed in Table II. The published Q value for $O^{16}(d,n)F_0^{17}$ reaction was used in the calibration of the spectrometer for the higher neutron energy data and the

TABLE I. Well-defined peaks in the PbO_2 target spectrum.

Observed neutron energy (Mev)	Identification	Half-width of peak (kev) Measured	Predicted
5.52	$F_{0,1}^{17}$	820[a]	320[b] ~820[c]
3.18	$N_{2,3}^{13}$	240	195[b] ~245[c]
2.62	F_2^{17}	180	185
0.63	F_5^{17}	90	70

[a] Solid curve.
[b] Assuming one neutron group only is present.
[c] The separation of the unresolved levels was added arithmetically to the value predicted assuming one neutron group only. Since this is a patently incorrect method of combining Gaussian curves, the apparent good agreement is misleading.

Q values obtained for the $O^{16}(d,n)F_2^{17}$ and $C^{12}(d,n)N_{2,3}^{13}$ reactions are relative to this. The disparity between the excitation energy for the $N_{2,3}^{13}$ group measured here and those reported previously[9] may be due to the relatively poor statistics.

IV. DISCUSSION

Adequate neutron flux is available to improve the resolution a factor of three by increasing the flight path by a factor of three. Further improvement might also be obtained by operating the cyclotron at low dee voltages, thus decreasing the width of the deuteron bursts. It appears feasible, therefore, to investigate even those (d,n) reactions for which the neutron groups are closely spaced in energy.

The chronotron offers perhaps the best timing precision presently available but it does suffer the considerable disadvantage that each event must be analyzed separately. Since the resolution of the spectrometer is determined primarily by the 4-mμsec width of the deuteron burst rather than by the method of timing the instrument is being converted to automatic recording using a time-interval to pulse-height converter[13] of resolution 1–2 mμsec. This simplifies considerably the measurement of (d,n) spectra and angular distributions while still permitting an accuracy not greatly different from that for charged particle reactions.

The excitation energies measured for the second and fifth excited states of the $O^{16}(d,n)F^{17}$ reaction agree reasonably well with the published values[11] obtained from the $O^{16}(p,p)$ and $O^{16}(p,\gamma)$ reactions. However, while the observed half-width of the second excited state is in agreement with published values it is perhaps significant that the observed half-width of the F_5^{17} group is only 90 kev (indicating that the natural width is somewhat less). This is in direct contradiction with the published values[11,14] of several hundred kev. It thus seems quite possible that the $(d_{\frac{3}{2}}^{+})$ single particle level (spin-orbit companion of the $(d_{\frac{5}{2}}^{+})$ ground state) which is expected to have a natural width of the order of 200 kev, may be found at an excitation energy slightly above 5 Mev. The rapid rise at the low end of the spectrum (F_6^{16} in Fig. 14) indicates a possible level which would be a likely candidate. This would be in better agreement with the corresponding $(d_{\frac{3}{2}}^{+})$ level in the mirror nucleus O^{17}. Further results obtained with the automatic recording spectrometer will be reported in *The Physical Review*.

TABLE II. Reaction Q values and corresponding excitation energies using the PbO_2 target.

	Reaction $C^{12}(d,n)N_{2,3}^{13}$	Reaction $O^{16}(d,n)F_2^{17}$	Reaction $O^{16}(d,n)F_5^{17}$
Measured neutron energy (Mev)	3.18±0.04	2.62±0.03	0.63±0.02
Assumed midtarget deuteron energy (Mev)	7.66±0.08	7.66±0.08	7.61±0.08[a]
Measured Q	−4.03±0.05	−4.66±0.06	−6.37±0.07
Calculated excitation energy[b]	3.75±0.05	3.03±0.06	4.74±0 07
Previous excitation energy (Mev)[c]	3.511 3.558	3.11	4.6,[d] 4.73[e]

[a] A shift in the deuteron energy occurred between the high- and low-energy runs.
[b] Calculated from the measured Q and published[9] ground-state Q for the given reaction.
[c] See reference 9.
[d] See reference 12.
[e] See reference 11.

V. ACKNOWLEDGMENTS

The authors wish to thank Mr. J. C. Hensel for his significant contribution to the work, and particularly for the design and construction of the high-voltage pulser. The assistance of Harvey M. Nye and Quin McLoughlin at various stages of the work is also acknowledged. It is a pleasure to thank Professor R. W. Pidd and Professor P. V. C. Hough for many helpful discussions, particularly while one of us (WCP) was on sabbatical leave.

[13] Weber, Johnstone, and Cranberg, Rev. Sci. Instr. 27, 166 (1956).
[14] H. L. Jackson and A. I. Galansky, Phys. Rev. 89, 370 (1953).